INVESTIGATIONS OF DIFFERENT DYE LASER CONCEPTS FOR COMBUSTION DIAGNOSTICS

DIPLOMA PAPER

HANS NEIJ
ANDERS NILSSON

Lund Reports on Atomic Physics, LRAP-104,
Lund, June 1989

CONTENTS

1. INTRODUCTION

This diploma work arose due to the demands of new dye laser types to be used in combustion diagnostics, preferably in CARS. Two different spectral characteristics were requested: a narrow-broadband output bandwidth of roughly 10 cm^{-1} and a broadband output with a mode separation of 8 cm^{-1}.
The main part of this work treats the measurements performed on the above mentioned projects and the consequent results. Introductorily CARS is presented, the real-world application of this work, followed by a description of basic laser theory. Finally a high pressure and temperature cell for CARS measurements is briefly presented.

2. CARS : A TOOL FOR COMBUSTION ANALYSIS

Due to the extraordinary characteristics of the laser light, lasers are frequently used for combustion diagnostics. There are three major techniques [1]:

- Laser-Induced Fluorescence (LIF)
- Raman Scattering
- Coherent anti-Stokes Raman Scattering (CARS)

The technique which is most commonly thought to have the largest potential for real flame diagnostics is CARS.

Coherent anti-Stokes Raman Scattering or CARS is especially powerful concerning measurements on combustional processes with a high degree of light emission (flames containing a lot of particles) which is the most common case in real-world situations. The advantage of CARS is that the information about the atoms and molecules at the measuring point is transmitted in the form of a laser beam. This property makes CARS particularly attractive as a diagnostic tool in harsh environments. The beam's coherent nature and conciderable signal strength facilitates the measurements.
The CARS effect may be described as an interaction of two photons from one laser beam at frequency ω_P and one photon from a laser beam at frequency ω_S through the third order non-linear susceptibility $\chi^{(3)}$ to generate an anti-Stokes photon at $\omega_{AS} = 2\omega_P - \omega_S$ [2-3] (Fig. 2.1.).

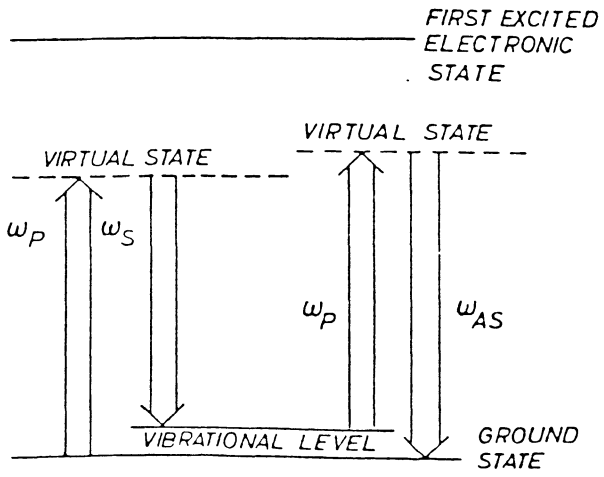

Fig. 2.1. Energy level diagram describing the CARS process.

In order to achieve high efficiency in the CARS process it is important to fulfill the phase-matching conditions which are illustrated in Figure 2.2.

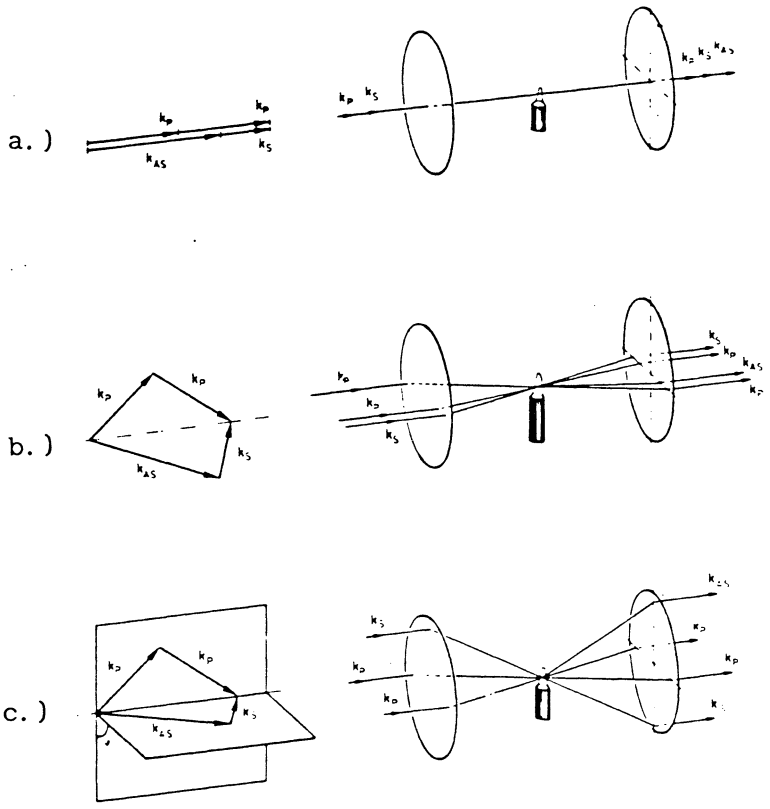

Fig. 2.2. Different phase-matching conditions.

The arrangements b.) and c.) in Figure 2.2. are called BOXCARS and folded BOXCARS, respectively, and are the most commonly used since they permit strong rejection of the laser beam by comparatively simple means. In conventional CARS the spectra are recorded through scanning the frequency of the Stokes beam ω_S, whereas the pump beam is held fixed at ω_P. Many laser shots are then necessary to create a complete spectrum. In this way CARS is only capable of being used in stationary media.

Using a broadband dye laser a complete CARS spectrum could be captured in a single laser pulse [4], which is particularly valuable when investigating turbulent media and ignition experiments. This technique utilizes one broadband ($\simeq$ 100 cm^{-1}) dye laser beam and one fix-frequency beam to generate a CARS beam as illustrated in Figure 2.3.

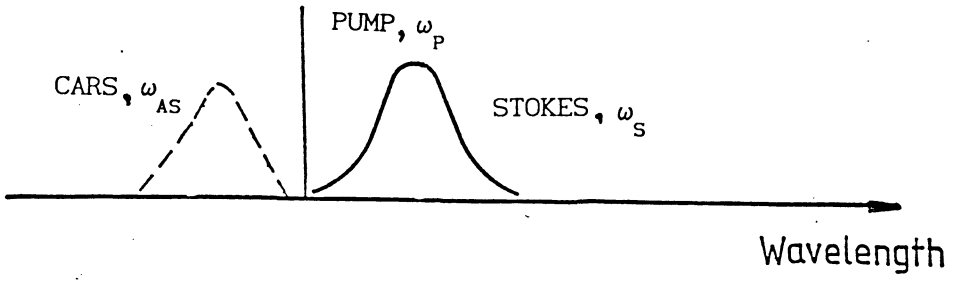

Fig. 2.3. CARS generation using one broadband beam and one narrowband fix-frequency beam.

A CARS spectrum is quite complex and for quantative measurements it is necessary to have a computer code for generating theoretical CARS spectra at various temperatures which are then fitted to experimental spectra.

There are two closely related CARS techniques:

- vibrational CARS
- pure rotational CARS

Probing of vibrational/rotational state populations using CARS is normally referred to as vibrational CARS and it is used for temperature measurements (Fig. 2.4.).

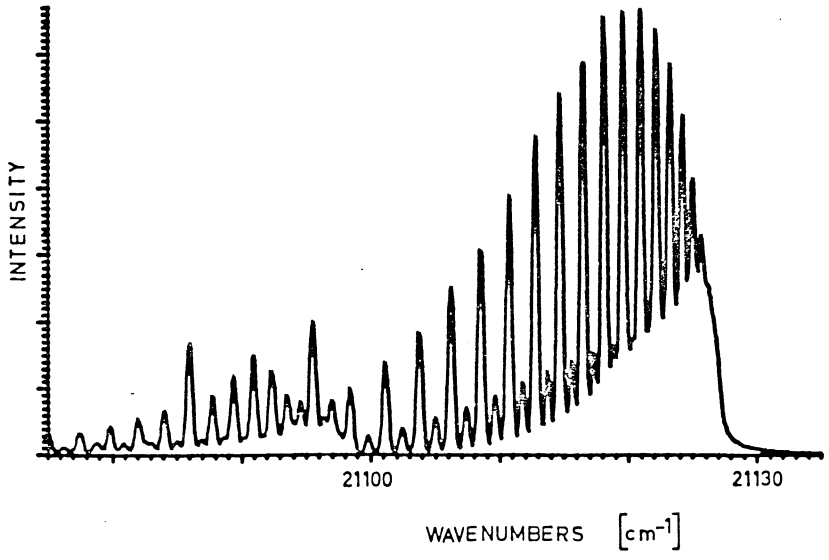

Fig. 2.4. Theoretical vibrational CARS spectrum for N_2 [1].

An alternative to vibrational CARS is to probe rotational transitions i.e. rotational CARS (Fig. 2.5.). Besides the advantage of an enhanced signal intensity, rotational CARS has a great potential since several species may be detected simultaneously using a broadband dye laser. Furthermore low temperatures can be measured with high accuracy. The largest drawback is the fact that the signal intensity is decreased more severely at higher tempeartures than in vibrational CARS. Therefore it would be desirable to combine rotational and vibrational CARS. In Ref. 11. it is shown that simultaneous rotational and vibrational CARS generation indeed is possible. In this case vibrational CARS may be used for measurements in the hot parts, while rotational CARS is used to probe the cooler parts.

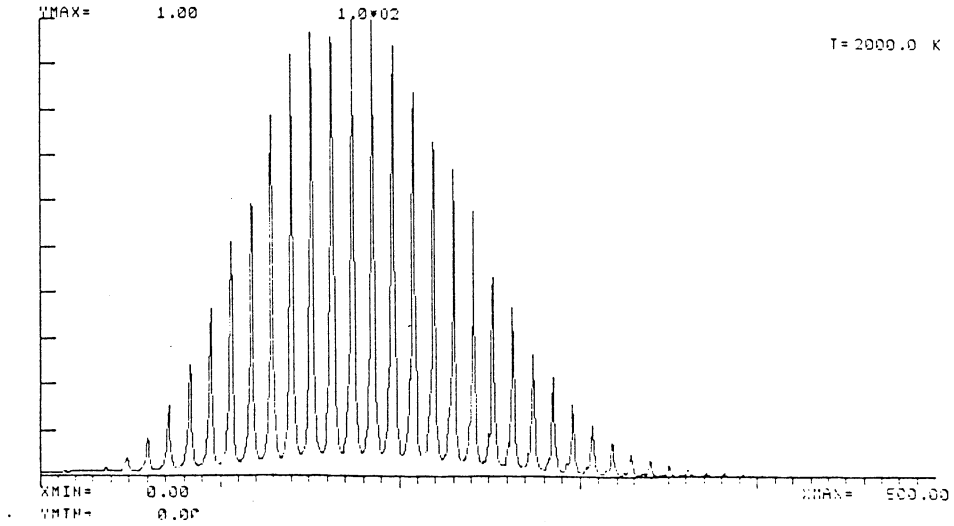

Fig. 2.5. Theoretical rotational CARS spectrum for O_2 [13].

3. LASER

A laser (Light Amplification by Stimulated Emission of Radiation) is a unique light source with a very narrow line-width and low beam divergence. Roughly, lasers can be divided into two categories: fix-frequency lasers and tunable lasers. As an example of fix-frequency lasers the Nd:YAG laser will be described in this work, whereas dye lasers represent tunable lasers [14,17,18].

3.1. THE LASER IDEA

Consider two arbitrary energy levels 1 and 2 of a given material and let N_1 and N_2 be their respective populations. If a plane wave with an intensity corresponding to a photon flux F is travelling along the z direction in the material, the elemental change of this flux due to both the stimulated emission and the absorption process in the shaded region of Fig. 3.1. is given by

$$dF = \sigma F (N_2 - N_1) dz$$

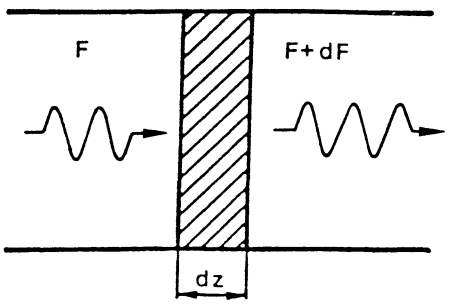

Fig. 3.1. Elemental change dF in the photon flux F for an e.m. wave when travelling a distance dz through the material.

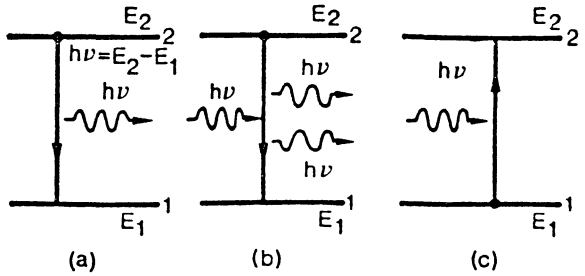

Fig. 3.2. Schematic illustration of the three processes: (a) spontaneous emission; (b) stimulated emission; (c) absorption.

The material behaves as an amplifier if $N_2 > N_1$. In this case we will say that there exists a *population inversion* in the material. Such a material is known as an *active material*.

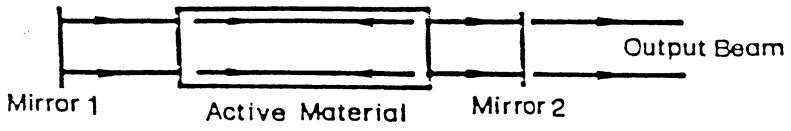

Fig. 3.3. Scheme of a laser.

Placing an active material in a resonant cavity, consisting of two mirrors, a plane e.m. wave travelling in a direction orthogonal to the mirrors will bounce back and forth between the two mirrors and be amplified, as mentioned above, on each passage through the active material. It is possible to extract a useful output beam if one of the mirrors is made partially transparent.

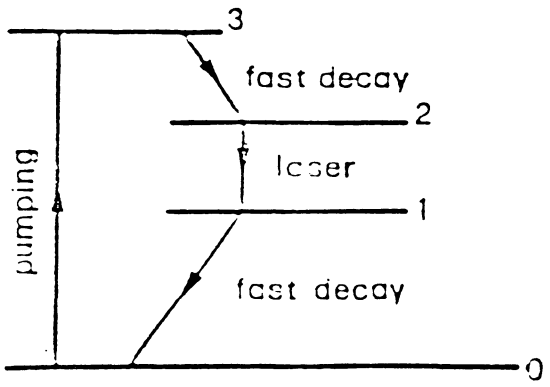

Fig. 3.4. Four-level laser scheme.

Let us consider an atom with four energy levels [18], see Fig. 3.4. To produce a population inversion, atoms (or molecules) are raised from the ground level 0 to level 3. If the atoms then decay rapidly to level 2, a population inversion can be obtained between levels 2 and 1. Once oscillation starts in such a *four-level laser*, however, the atoms will be transferred to level 1 (due to stimulated emission), and decay rapidly to level 0.

The process by which atoms are raised from level 0 to level 3 is known as *pumping*. There are several ways in which this

process can be realized in practice, e.g. some sort of lamp of sufficient intensity, by an electrical discharge in the active medium or by a laser.

If a system will work in a four-level scheme or whether it will work at all depends on whether the various conditions given above are fulfilled and if the laser gain exceeds the cavity loss.

3.2. FIX-FREQUENCY LASER

One of the most important pulsed fix-frequency lasers is the Nd:YAG laser. In this laser system neodym ions are doped in yttrium aluminum garnet YAG. The Nd:YAG is a four level laser, which means that the Nd^{+3} ions are excited by a flash-lamp.

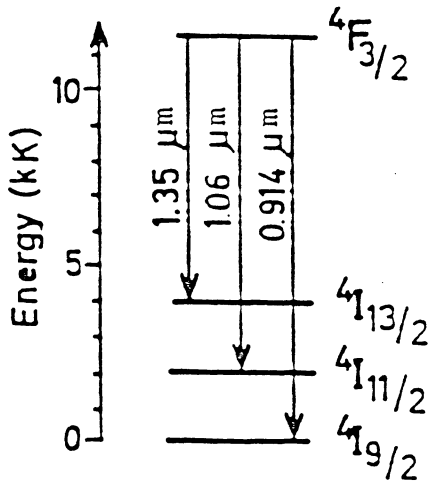

Fig. 3.5. The transitions for the Nd:YAG laser.

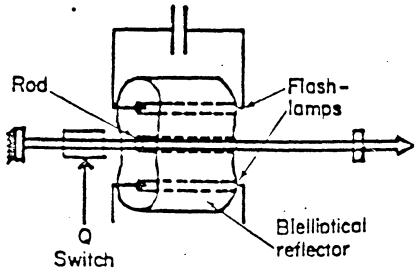

Fig. 3.6. Nd:YAG laser.

Fig. 3.6. shows a typical pumping arrangement. Here the laser rod is placed along one focal line of an elliptical reflector and the pumping lamp is placed at the other focal line. This concentrates the light of the flashlamp onto the laser rod. Most commercial Nd:YAG systems use an oscillator and one or two amplifiers to achieve a narrow linewidth and a fine mode structure.

As an typical example; a Nd:YAG system for spectroscopy produces 1 J pulses in 10 ns at 1.06 μm, with a repetition rate of 10 Hz. Using frequency doubling techniques the 1.06 μm line can be transformed to 532 nm.

3.3. DYE LASERS

Organic dyes are large and complicated molecular systems containing conjugated bonds. Usually they have strong absorption bands in the UV or the visible range of the spectrum, and when excited by light of appropriate wavelength, they display intense broad-band fluorescence spectra, such as shown in Fig. 3.7. for Rhodamine 6G in ethanol solution.

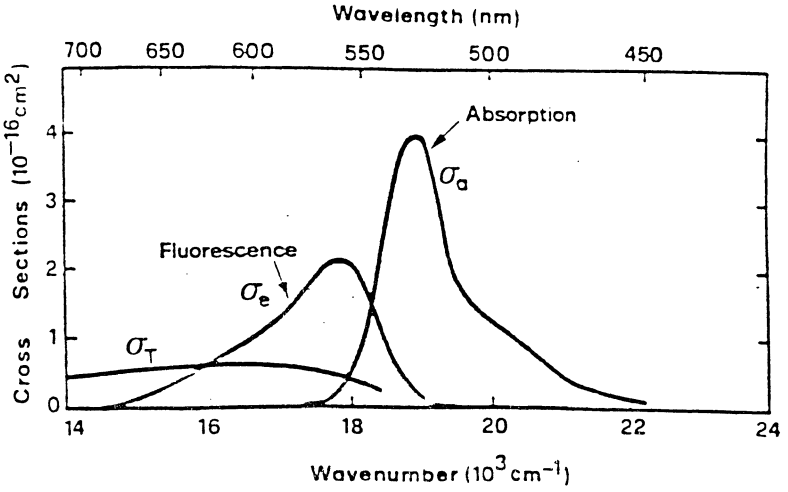

Fig. 3.7. Absorption cross section σ_a, stimulated-emission cross section σ_e (singlet-singlet transition) and absorption cross section σ_T (triplet-triplet transition) for an ethanol solution of Rhodamine 6G [18].

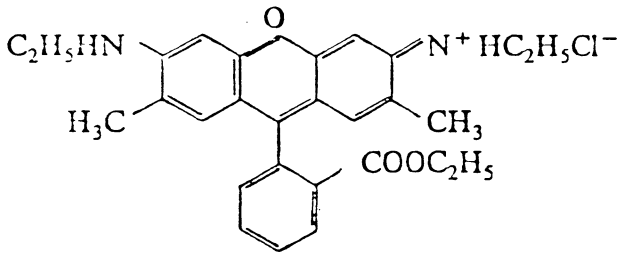

Fig. 3.8. As an example, the structural formula for the widely-used dye Rhodamine 6G (xanthene dye) [18].

Each electronic state is actually made up of a set of vibrational levels and rotational levels. The separation between vibrational levels are typically 1400-1700 cm^{-1}, whereas the separation of rotational levels is typically 100 times less. Since the broad-banding mechanism is much more important in liquids than in solids, the rotational lines are not resolved and therefore give rise to a continuum of levels between the vibrational levels.

Interaction with electromagnetic radiation can raise the molecule from the ground singlet level S_0 to one of the vibrational levels of the excited S_1 level. Once in the excited state the molecule decays in a very short time (non-radiative decay, $\tau_{nr} \simeq$ picoseconds) to the lowest vibrational state of the S_1 level. From there it decays radiatively to some vibrational level of S_0 (*fluorescence*). This fluorescent emission, will take form of a broad and featureless band shifted to the long-wavelength side of the absorption band. Having dropped to an excited rotational-vibrational state of the ground level S_0, the molecule will then return to the lowest vibrational level by a further very fast (of the order of picoseconds) non-radiative decay.

When the molecule is in the lowest level of S_1, it can also decay to level T_1 (triplet). This system is called *intersystem crossing* and is caused by collisions and is in some cases troublesome, since the fluorescent light from the singlet state may to some extent be absorbed by the triplet state. The lifetime of the triplet state is rather long $\simeq \mu s$

and weak radiative transitions yield phosphoresence.

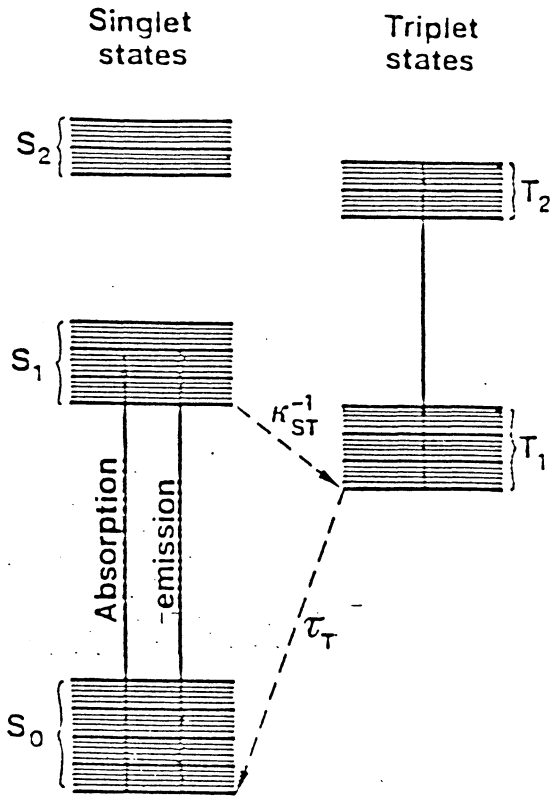

Fig. 3.9. Typical energy levels for a dye solution. The singlet and triplet levels are shown in separate columns.

If the organic dye solution is enclosed in a cell, placed in a laser cavity, and sufficient pump-power is supplied, we will have lasing. Using ordinary broadband laser mirrors stimulated emission in a spectral range of about some twenty or thirty Ångström will occur. A very important step were taken 1967 by Soffer and McFarland who replaced the totally reflecting mirror by a reflection grating in Littrow mounting, Fig. 3.10. This decreased the linewidth for the stimulated emission to about 0.5 Å. By rotating the grating, the laser could continuously be tuned.

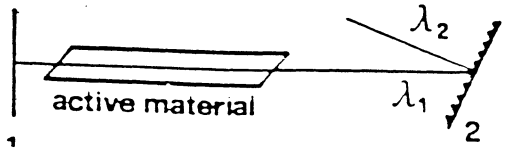

Fig. 3.10. A laser using the wavelength dispersive behavior of a reflection grating.

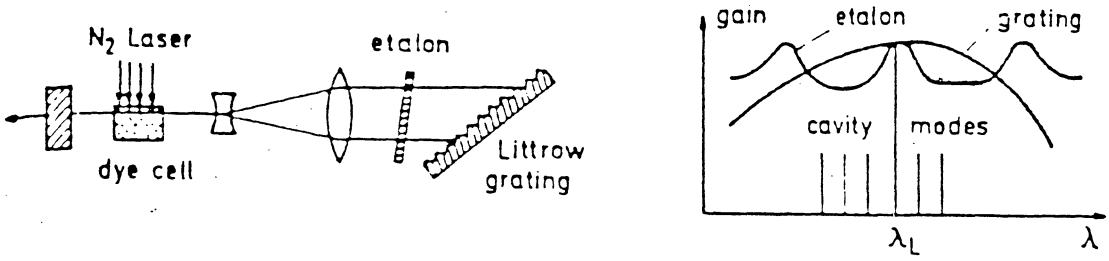

Fig. 3.11. Dye laser of Hänsch type.

By using a telescope expanding the beam, a larger part of the grating can be illuminated. This increases the resolving power of the grating and the linewidth is limited to about 0.05 Å. Inserting an intra cavity etalon reduces the linewidth by a factor 10, Fig. 3.11.

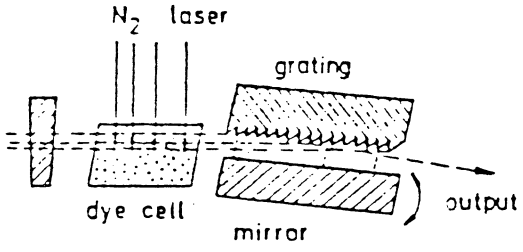

Fig. 3.12. A Littman cavity.

Fig. 3.12. shows a Littman cavity. In this arrangement no beam expander is used. A fixed grating is working at grazing incidence and the laser is tuned by rotating a mirror, reflecting the 1st order of the grating. The output beam can be extracted in the 0th order of the grating (reflection). Alternatively, tuning and spectral narrowing may be achieved by one or more prisms in the laser cavity. The relatively small angular dispersion of a single prism is sufficient to

isolate one or several sharp lines in gas lasers, for example, where this method has long been used. But it gives hardly any reduction in spectral bandwidth of a dye laser, so that multiple-prism arrangements have to be used.

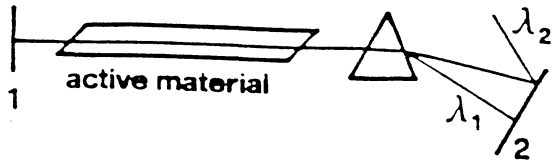

Fig. 3.13. A laser using the wavelength dispersive behavior of a prism.

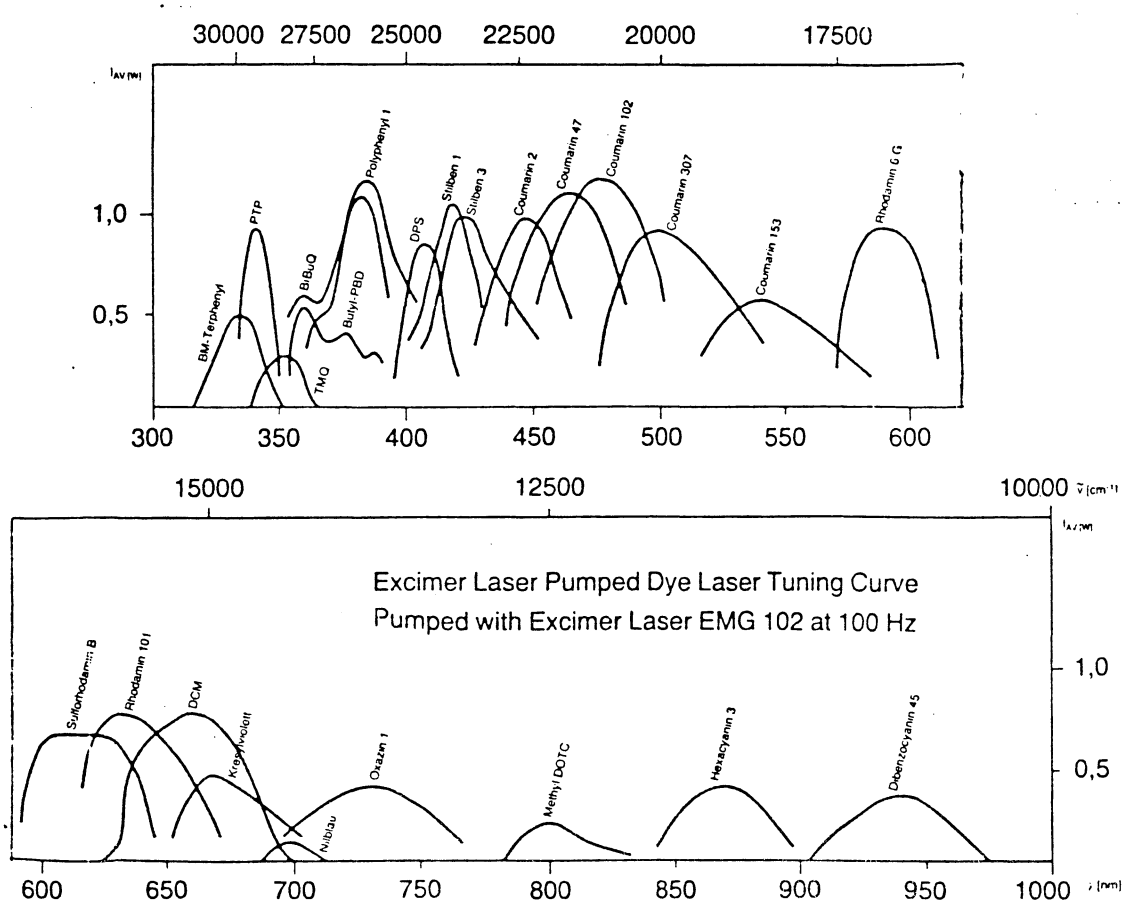

Fig. 3.14. A spectral range from 320 to 1000 nm is available using different dyes [2].

Dye lasers are usually pumped by pulsed fix-frequency lasers, such as N_2 lasers, excimer lasers or a frequency doubled Nd:YAG laser, but also a pumped flashlamp can be used. If high pulse energy is desired at the same time as narrow linewidth and small beam divergence, an oscillator-amplifier arrangement is used, see Fig. 3.15.

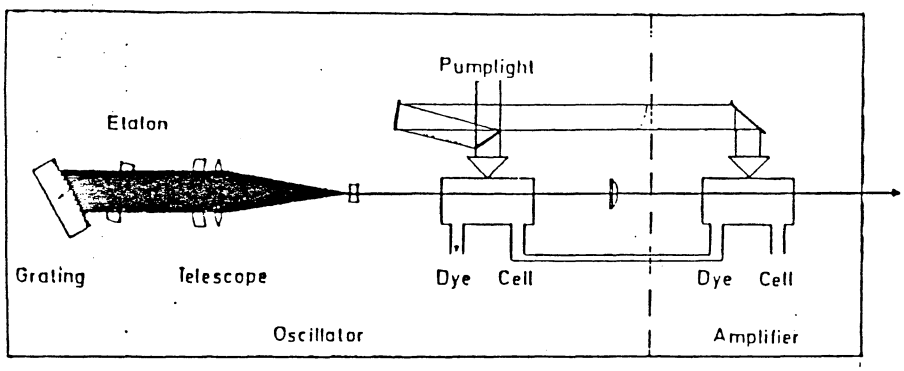

Fig. 3.15. Narrow band tunable dye laser system. Note the oscillator-amplifier configuration.

4. A NARROW-BROADBAND DYE LASER

4.1. EXPERIMENTAL IDEA

When employing the broadband dye laser techniques for generating vibrational CARS spectra mentioned in Chapter 2. one squanders most of the energy from the dye laser, as only a width of about 10 cm^{-1} is used in the transition. The rest of the broadband profile of approximately 100 cm^{-1} is of no importance. Therefore it would seem judicious to try to concentrate the energy from the dye laser into a width of roughly 5-10 cm^{-1}.

The intensity of the CARS beam is proportional to the square of the distance the pump and the Stokes beams are overlapping in Fig. 2.2. (normally about 1 mm). The angle between these beams determines the resolution. A large angle gives a high spatial resolution which is appreciable in turbulent media. Building a narrow-broadband dye laser constitutes a method for eating the cake and having it i.e. to achieve a high signal strength, enabling measurements in flames with low transmission, and an enhanced spatial resolution.

Inserting a dispersive element into the cavity of a dye laser could be a possible means to achieve a spectral condensation, i.e. reducing the bandwidth of the output signal while the energy of the beam remains much the same [22]. It would be desirable to attain bandwidths of about 5 to 10 cm^{-1} by using dispersing prisms in the cavity.

The purpose of this investigation was to determine to what extent this worked and, if getting promising results, discover the proper distances between the components of the dye laser, what kind of prisms that were auspicious, what angle of incidence that was to be used and the influence of the concentration of the dye on the dye laser output. Summarizing this work it should be possible to give recommendations on the number of prisms necessary to achieve a certain bandwidth and the maximum beam energy at this bandwidth.

4.2. DISPERSING PRISMS

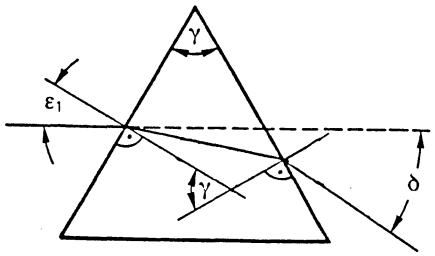

Fig. 4.1. Geometry of a dispersing prism.

A ray entering a dispersing prism, as in Fig. 4.1., will emerge having been deflected from its original direction by an angle δ known as the angular deviation. δ increases with the index of refraction n which is a function of frequency. For most transparent dielectrics of practical concern $n(\lambda)$ decreases as the wavelength increases across the visible (Fig. 4.2.). Clearly then $\delta(\lambda)$ will be less for red light than it is for blue.

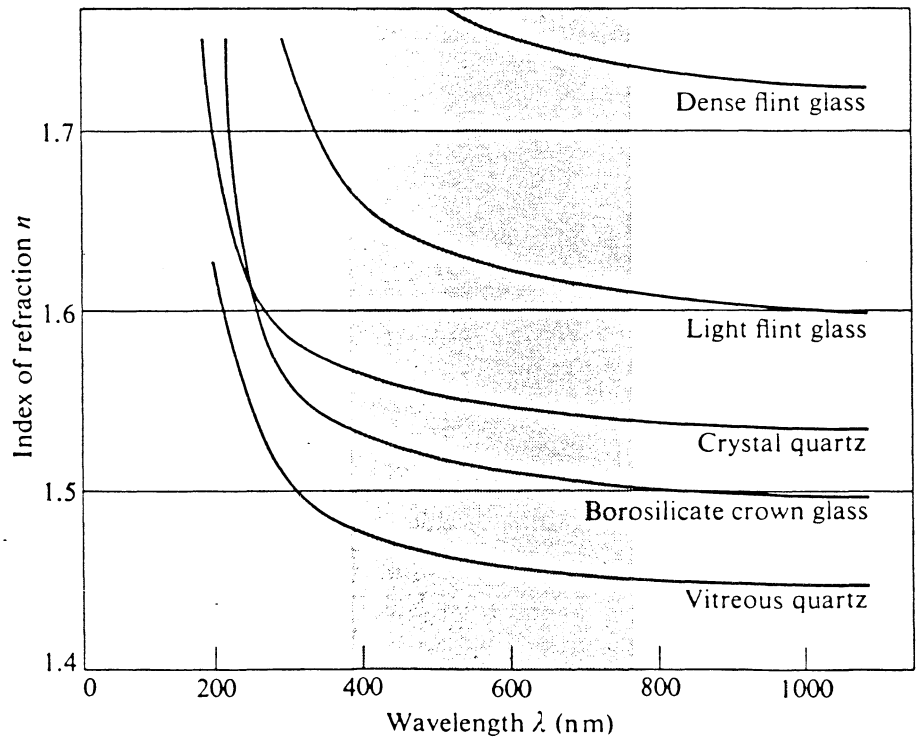

Fig. 4.2. The wavelength dependence of the index of refraction for various materials [21].

A plot of the angular deviation as a function of the angle of incidence ε_1 is shown in Fig. 4.3. The smallest value of δ is known as the minimum deviation δ_m. It can also be shown that the ray, for which the deviation is a minimum, traverses the prism symmetrically i.e. parallell to its base.

Combining Snell's law with geometrical considerations leads to the equation relating the index of refaction to the minimum deviation

$$n = \frac{\sin\left(\frac{\delta_m + \gamma}{2}\right)}{\sin\frac{\gamma}{2}}$$

where γ is the apex angle.

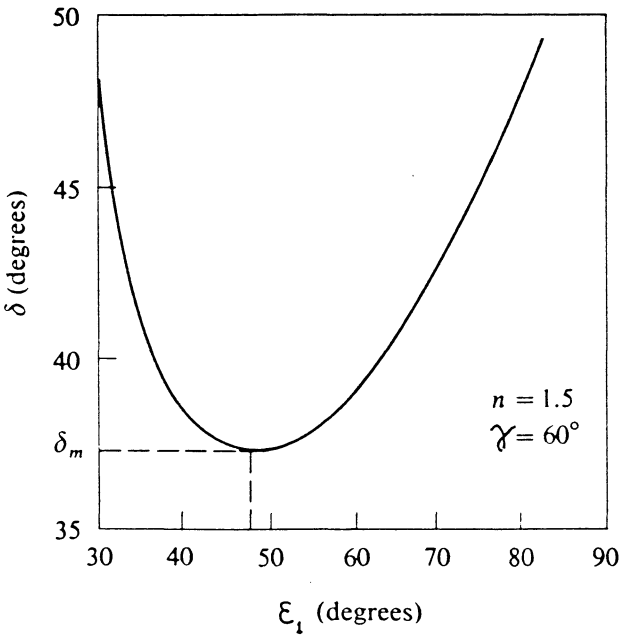

Fig. 4.3. Deviation versus incident angle.

4.3. EXPERIMENTAL SET-UP

The experimental set-up is schematically shown in Fig. 4.4. The dye laser was pumped by a Nd:YAG laser emitting vertically polarized light at a wavelength of 532 nm and a repetition rate of 10 Hz. This light was first deflected via a beamsplitter transmitting 50% and then via another beamsplitter transmitting 90%. In this manner the energy of the beam used for pumping the dye laser was set at 12 mJ. The light was focused on the dye cell by a cylindrical lens with a focal length of 200 mm.

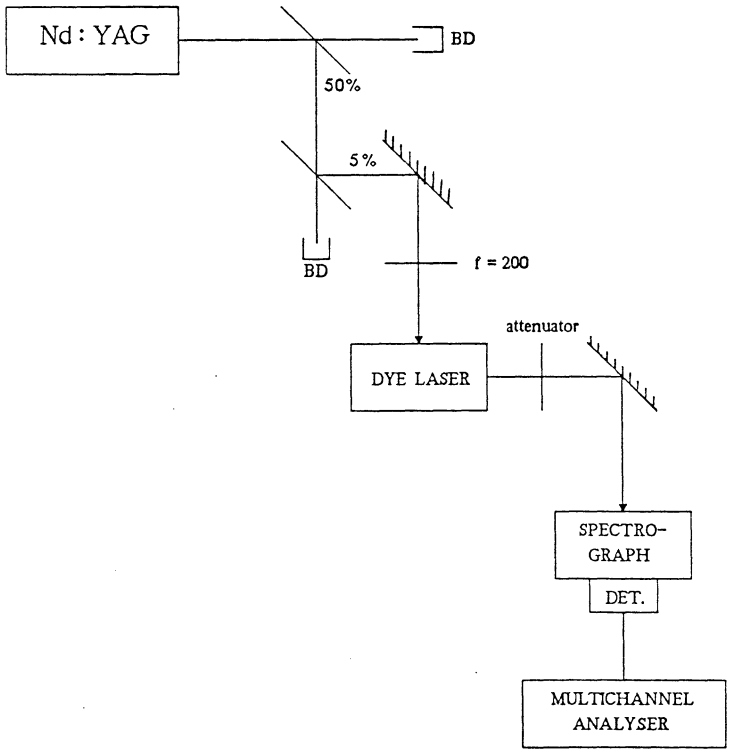

Fig. 4.4. Experimental set-up.

The beam from the dye laser was adequately attenuated with neutral density filters before entering the spectrograph through an entrance slit of 25 μm. The spectrograph (Jarrel-Ash model 1233/1234) had three different gratings of which only the third with a dispersion of 1.5 nm/mm was used. As a detector we used a diode array (Tracor Northern 6100 series) with a light sensitive area of (25 x 2.5) mm and 1024 individual elements. The spectrum was dispersed onto the

detector and consequently displayed on the screen of the multichannel analyser (Tracor Northern TN-1710). The exposure time was set to 100 ms equivalent to the repetition rate of the Nd:YAG laser.

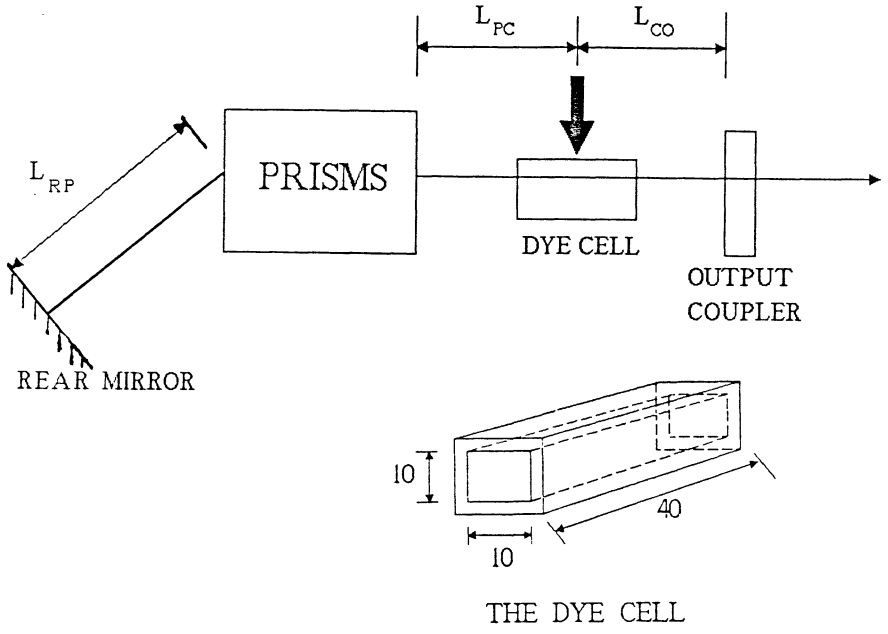

Fig. 4.5. Dye laser arrangement.

A sketch of the dye laser is shown in Fig. 4.5. A mirror with a minimum reflective power of 99% was used as a rear mirror. In order to be able to wavelength calibrate the dye laser output with the sodium lines we were inclined to choose a dye lasing at approximately 580-600 nm. The dye chosen was KITON RED 620 dissolved in EtOH yielding a concentration of 130 mg/l. This solution was pumped through the dye cell by a Quantelpump (DCP 02) with a capacity of 90 l/h. The internal dimensions of the cell was (10×10×40) mm. The cell was tilted at Brewster's angle to attain vertically polarized laserlight from the dye cell and to eliminate Fabry-Perot effects from the parallell walls of the cell. Either a wedge or a glass plate (thickness 12.8 mm) was employed as an output coupler.

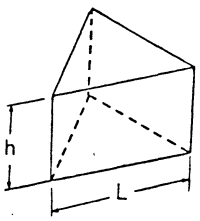

The prisms used were all equilateral 60°-prisms with the dimensions h × L = (30 × 30) mm.

When lining up the dye laser a Helium-Neon laser was used. At first we used a Coherent 210 as power meter but its lack of precision made us change to a Scientech 362.

4.4. MEASUREMENTS AND RESULTS

4.4.1. CALIBRATION

The sodium D-lines were used for calibrating the arrangement of the spectrograph and the optical multichannel analyser. A sodium lamp was placed in front of the slit of the spectrograph and the two peaks were displayed on the screen of the multichannel analyser. The number of channels separating the peaks were measured to be 28. Since the distance between the lines D_1 and D_2 is known to be 5.97 Å we calculated the spacing of one channel to be equivalent to 0.2132 Å. This gauging was performed twice a day during the experiment yielding the same result.

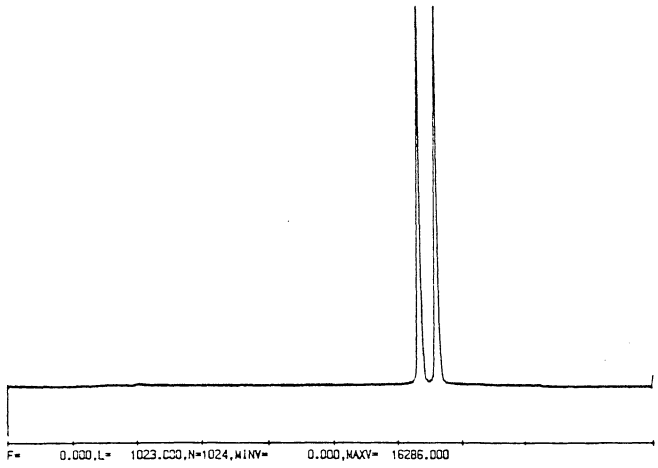

Fig. 4.6. The sodium D-lines used for calibration.

4.4.2. CHOOSING AN OUTPUT COUPLER

When the output coupler consists of a plain glass plate one has the disadvantage of possible Fabry-Perot effects from the parallel sides of the plate. On the other hand the cavity is very easily lined up with for example a Helium-Neon laser.
By using a wedge one eliminates the Fabry-Perot effects but problems arise when lining up the dye laser.

Comparing the spectral characteristics of the output beam when using either a glass plate or a wedge no difference in FWHM (the full width at half maximum) was seen. However when comparing the output energies of the dye laser a reduction of about 20% was indicated when using the wedge.
As the Fabry-Perot effects were not that striking and at times even not visible we choose to employ the glass plate as our output coupler.

4.4.3. A DYE LASER CAVITY WITHOUT PRISM

The energy and the full width at half maximum of the output from the dye laser were measured as a function of the total cavity length. The result is shown graphically in Fig. 4.7.
It was also proved that the arrangement of the rear mirror and the output coupler did not in any way affect the result, i.e. the total length determines both the FWHM and the output energy.

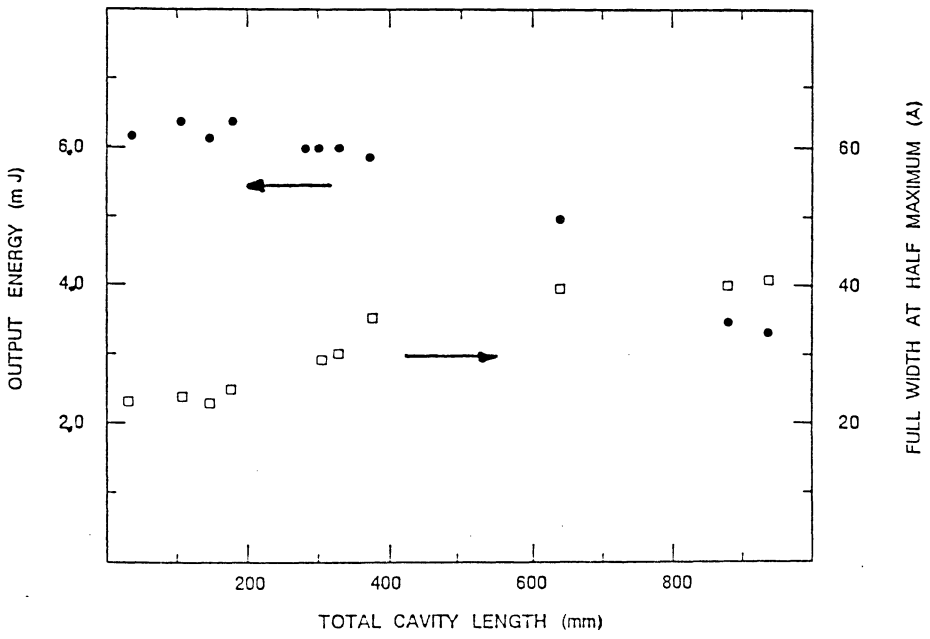

Fig. 4.7. Energy (●) and full width at half maximum (□) of the dye laser output as a function of the total cavity length.

4.4.4. RELATION BETWEEN PUMPING ENERGY AND DYE LASER OUTPUT

In order to investigate the relationship between input and output energies and also to verify that the dye was not saturated at the pumping energy of 12 mJ the pumping energy was reduced by half. The output energy was then likewise reduced by half. The FWHM was sligthly increased (by maximum 10%). This proved that the dye was not saturated at 12 mJ.

4.4.5. DISTANCE BETWEEN OUTPUT COUPLER AND DYE CELL

When having one prism in the cavity and changing the distance L_{co} in Fig. 4.5. it was found that when this distance decreased, so did the FWHM and the output energy. The output energy did, however, not decrease as drastically as the FWHM. This led us to the decision of placing the output coupler as close to the dye cell as possible i.e. $L_{co} = 50$ mm.

4.4.6. DISTANCE BETWEEN DYE CELL AND PRISM

When using one prism in the cavity and increasing the distance L_{pc} in Fig. 4.5. an enhancement of the FWHM and a decrease of the dye laser output energy were experienced. Due to practical inconveniences it was not possible to reduce the distance L_{pc} to less than 150 mm.

4.4.7. DISTANCE BETWEEN THE INDIVIDUAL PRISMS

No significant differences in either FWHM or output energy were established when varying the spacing separating the prisms. The configuration used in future experiments was chosen on practical grounds (Fig. 4.8.).

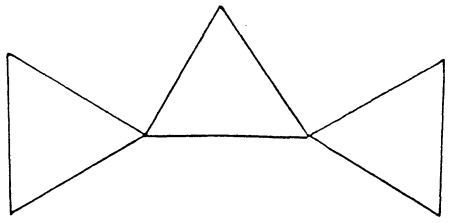

Fig. 4.8. Configuration of the prisms.

4.4.8. DISTANCE BETWEEN PRISMS AND REAR MIRROR

One prism

When changing the distance L_{rp} in Fig. 4.5. a minimum in the FWHM was found at approximately 120 mm while the output energy was declining with the distance (Fig. 4.9.).
At very short distances between prism and rear mirror (≃40 mm) the dye laser signal was spectrally distorded and therefore difficult to examine.

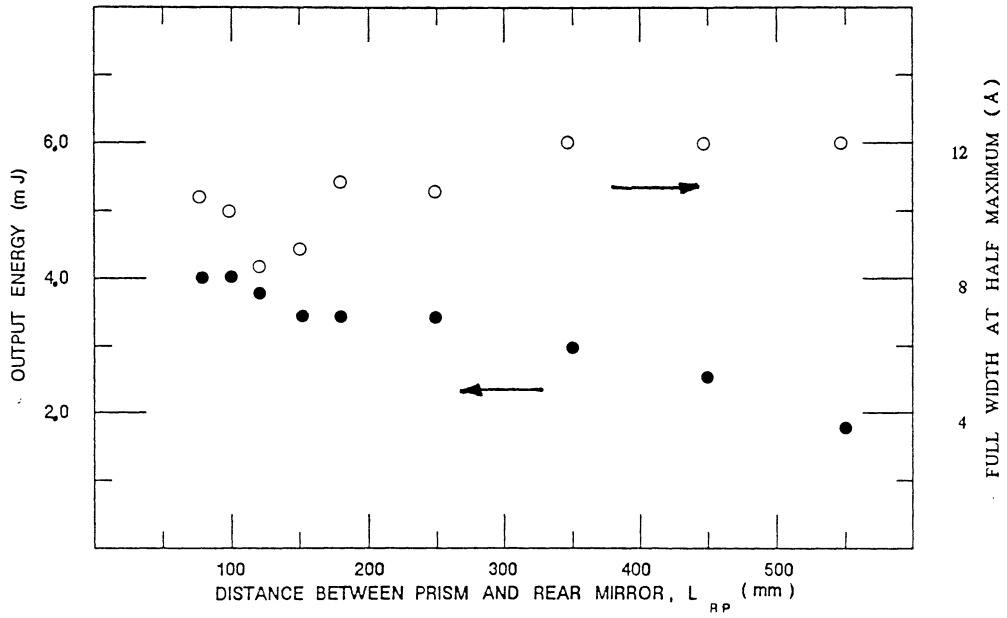

Fig. 4.9. Full width at half maximum (○) and output energy (●) versus distance between prism and rear mirror when using one F2-prism in the dye laser cavity.

Two prisms

The minimum in FWHM was now observed at L_{rp} = 110 mm. The output energy still showed a decline with the distance.

Three prisms

The same results as when utilizing one or two prisms were established but for the fact that the distance giving rise to a minimum in FWHM was approximately 100 mm.

4.4.9. CHOICE OF PRISMS

Three different types of prisms were employed as dispersing elements in the cavity. Table 1. shows the results achieved using one prism and the optimum distances stated above.
As we only had access to one prism of type SF10 the rest of the measurements were done utilizing prisms of type F2. It seems as if utilizing SF10 would result in an additional spectral condensation due to the higher angular dispersion of this glass in the wavelength region studied.

Table 1. The influence of different prisms on output energy and full width at half maximum. The index of refraction is given at λ = 589 nm.

PRISM	INDEX OF REFRACTION	RELATIVE ANGULAR DISPERSION	FWHM (A)	ENERGY (m J)
Quartz glass	1.46	1.0	26	3.5
Flint glass, F2	1.62	3.0	8.5	3.8
Dense flint glass, SF10	1.73	5.3	6.5	3.6

4.4.10. ANGLE OF INCIDENCE

Varying the angle of incidence ε_1 in Fig. 4.1. no noticeable differences in either FWHM or dye laser output energy were noticed. Again for practical reasons the prisms were arranged for the beam to traverse them symmetrically (i.e. minimum deviation).

4.4.11. OPTICAL PATH LENGTH WITHIN THE PRISMS

It was noticed that the farther the beam travelled within the prisms the higher energy and the narrower output spectra were measured. Another phenomenon disclosed was an increasing sensitivity to adjustments when shortening the optical path length within the prisms.

4.4.12. NUMBER OF PRISMS

Table 2. The results are shown when utilizing one, two or three F2-prisms placed giving minimum deviation and as long an optical path length as possible at the optimal distances between the components of the dye laser. The pumping energy was 12 mJ.

NUMBER OF PRISMS	FWHM (Å)	ENERGY (mJ)
1	8,5	3,8
2	4,3	2,7
3	3,2	1,5

4.4.13. SINGLE-MODE VERSUS MULTI-MODE PUMPING

No significant differences in FWHM or output energy were detected between pumping the dye cell with a single-mode or a multi-mode Nd:YAG laser.

4.4.14. TUNING WITH THE REAR MIRROR

The components of the dye laser were placed at their optimal positions. Prisms made of flint glass (F2) were utilized. The dye cell was pumped with an energy of 12 mJ. The tuning of the dye laser was performed by adjusting the rear mirror.
The grating of the spectrograph was limiting the measurements to that extent that it was only possible to study the spectral contents of the dye laser output up to λ = 5929 Å.
In Figures 4.10. and 4.11. the results are shown graphically when tuning with either two or three prisms in the cavity. The FWHM for different regions is also marked in the graphs. The tuning range is at least 120 Å in both cases which could be compared to the FWHM when not having any prisms in the cavity. This width is roughly 30 Å at the same total cavity length ($\approx$ 300 mm) which indicates the tuning profile not to coincide with the lasing envelope.

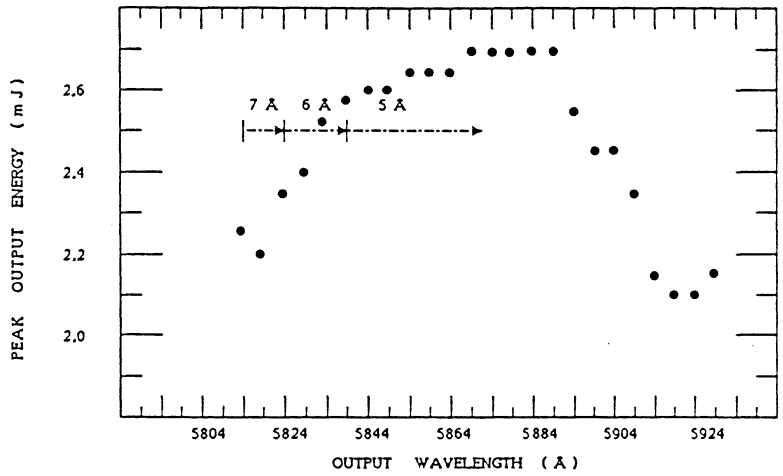

Fig. 4.10. The output energy when tuning the dye laser containing two F2-prisms. The FWHM for different regions is indicated.

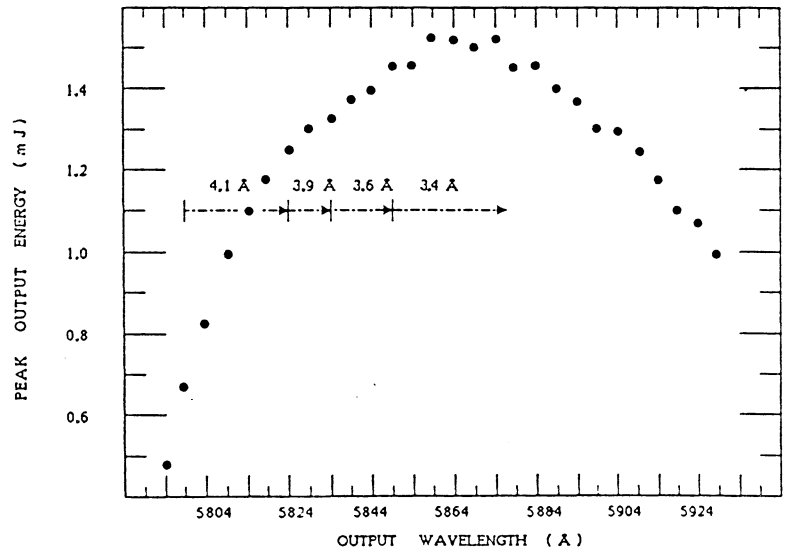

Fig. 4.11. The output energy when tuning the dye laser containing three F2-prisms. The FWHM for different regions is indicated.

4.4.15. POLARIZATION OF THE PUMPING LIGHT

The polarization of the pumping light was altered by inserting a $\lambda/2$-plate in the beam from the Nd:YAG laser. When the polarization coincided with the inclination of the dye

cell the output energy was vertically polarized and reaching its maximum. If the polarisation was shifted 90°, the output energy was horisontally polarized and minimized. The ratio between maximum and minimum energies was roughly 1.7 while the FWHM remained unaltered.

4.4.16. DYE CONCENTRATION

A solution with a concentration of 1 mg KITON RED 620 per ml EtOH was prepared. It was added by instalments to 500 ml EtOH. The concentration of the dye solution used was given by

$$y = \frac{1000X}{500+X} \text{ (mg/l)}$$

where x is the added amount of concentrated dye solution (mg). The solution was pumped through the dye cell and used in two different arrangements.

Firstly in a cavity without prisms and a total length of 300 mm where the central wavelength, the FWHM and the output energy were investigated. The results of the first set-up are shown in Figures 4.12.a) and 4.12.b).

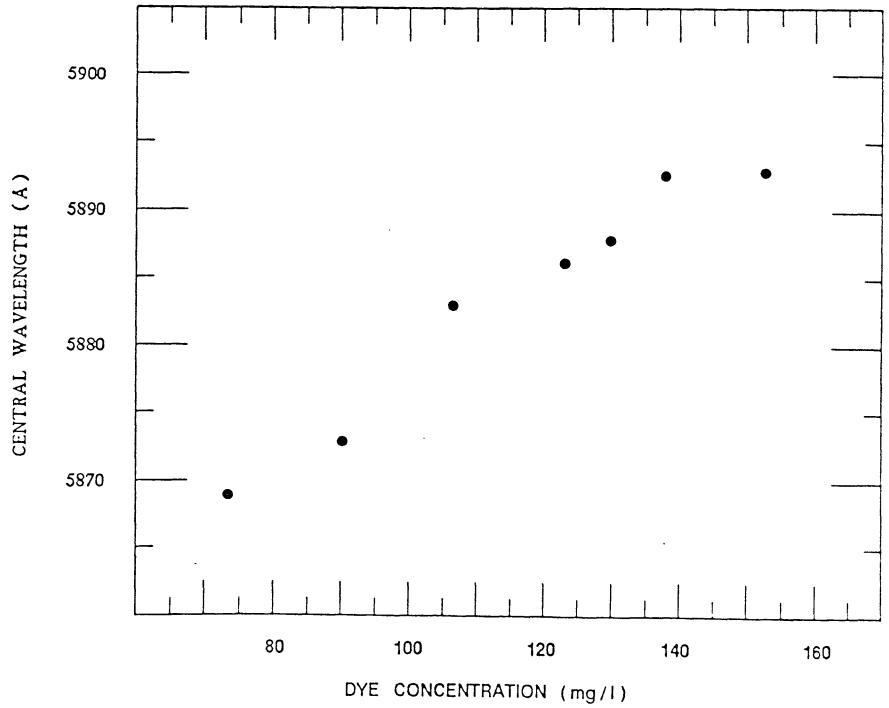

Fig 4.12.a) The influence of the dye concentration on the central wavelength of the dye laser output, when using a cavity without prisms.

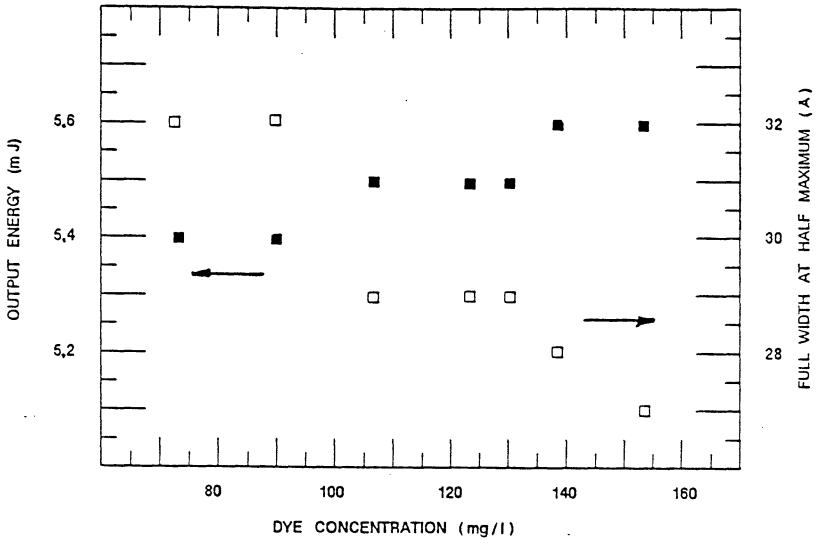

Fig. 4.12.b) The influence of the dye concentration on FWHM (□) and output energy (■), when using a cavity without prisms.

The second set-up was composed by a cavity with two prisms (F2) in the previously mentioned optimal lengths and dispositions. The central wavelength was set at 5874 Å and the FWHM and the energy were measured. There was no detectable difference in FWHM but the dye laser energy was increasing with the concentration as pictured in Fig. 4.13. Studying this graph it seems as if the previously used concentration of 130 mg/l EtOH giving an output energy of 2.7 mJ was a reasonable choice.

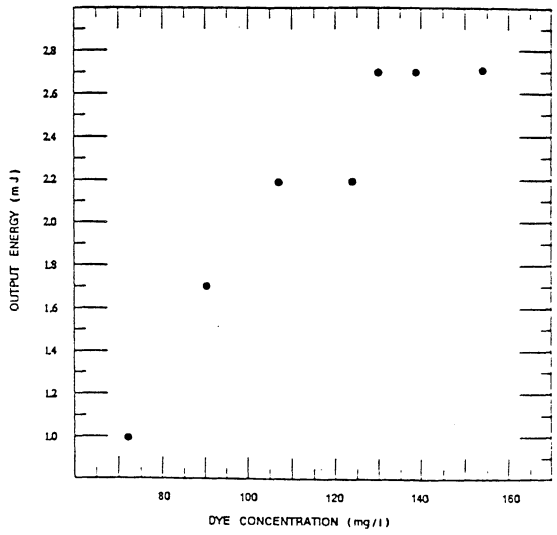

Fig. 4.13. The influence of the dye concentration on the output energy, when using two prisms in the cavity.

4.4.17. REFLECTIONAL LOSSES

To estimate the reflectional losses when inserting a prism into the cavity the Fresnel equations come handy.

$$r_{\perp} = \frac{n_i \cos \varepsilon_i - n_t \cos \varepsilon_t}{n_i \cos \varepsilon_i + n_t \cos \varepsilon_t} \qquad R_{\perp} = r_{\perp}^2$$

where n_i = index of refraction for the incident medium
n_t = index of refraction for the transmitting medium
ε_i = angle of incidence
ε_t = angle of transmission
$R_{\perp}$ = reflectance for the vertically polarized light

When using $\varepsilon_i = 48^{\circ}$, the angle of incidence yielding minimum deviation in the F2-prisms, and assuming n_i and n_t to be independent of the wavelength in the region studied one gets $R_{\perp}$ to be equal to 0.174. The total reflectional loss is given by $1-(1-R_{\perp})^{2N}$ where N is the number of prisms used.
Table 3. shows that the empirical losses were of the same magnitude as the theoretical losses which indicates the use of the Fresnel equations to be legitimate. There should, however, also exist losses due to absorption within the prisms.

Table 3. A comparison of the empirical and theoretical reflection losses when inserting prisms in the cavity.

NUMBER OF PRISMS	THEORETICAL REFLECTION LOSSES	EXPERIMENTAL REFLECTION LOSSES
1	0,32	0,31
2	0,53	0,51
3	0,68	0,73

Returning to the other part of the Fresnel equations

$$r_{\parallel} = \frac{n_t \cos \varepsilon_i - n_i \cos \varepsilon_t}{n_i \cos \varepsilon_t + n_t \cos \varepsilon_i} \qquad R_{\parallel} = r_{\parallel}^2$$

and calculating the reflection of the component polarized vertically to the one considered above one gets $R_{||}$ to be equal to 0.00148. By this, one would anticipate a possible means to increase the output effect and thereby ameliorate the spectral condensation by arranging the prisms vertically.

4.4.18. VERTICAL ARRANGEMENT OF THE PRISMS

Experiments were made with the prisms arranged vertically as pictured in Fig. 4.14. The same distances and configurations as in the horisontal arrangement were used.
The energy of the dye laser was indeed increased but to a evanescent extent, only 20%. At the same time the FWHM was increased with at least a factor two.
An explanation to this strange behavior has not been found. The experiments with this set-up were not further pursued.

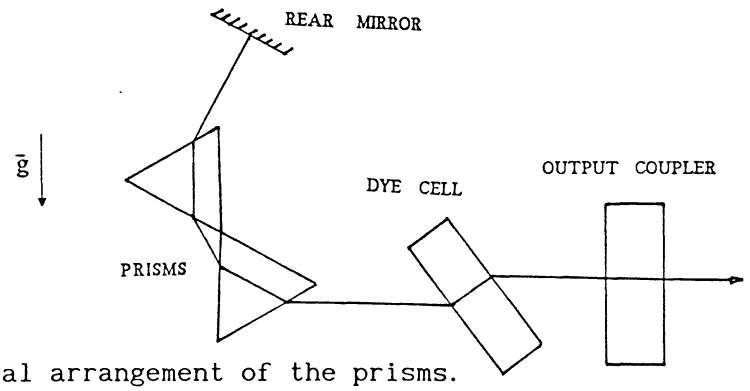

Fig 4.14. Vertical arrangement of the prisms.

4.4.19. TEMPORAL DRIFT

In order to estimate the temporal drift of the output peak of the dye laser 100 scans were summarized on the multichannel analyser and the central wavelength was measured. This experiment was repeated every 20 minutes. The pumping Nd:YAG laser was not switched off between the measurements in order to eliminate instabilities due to warming-up effects.
During a period of five hours the central wavelength of the peak never varied more than ± 0.6 Å. The momentary change of the peak wavelength however was as large as ± 0.9 Å.

4.4.20. SPECTRAL CONTENTS OF THE DYE LASER BEAM

The mirror reflecting the dye laser light onto the slit of the spectrograph was adjusted depicting different parts of the beam on the slit.
The peak value was distinct but when moving the beam across the slit there were measurable peaks over a range of roughly 3 Å. The total spectral contents of the beam extended over approximately 8.5 Å. If this should cause a problem it could be eliminated by placing a diaphragm outside the dye laser, thereby also excluding a small part of the output energy.

4.4.21. SPECTRAL PROFILES OF THE DYE LASER OUTPUT

By comparing the averaged spectra (100 scans) collected when utilizing a dye laser cavity without prisms and a total cavity length of 300 mm with Gaussian curves with identical amplitudes and widths a satisfactory agreement was found (Fig. 4.15.). For single-shot profiles there were larger deviations from ideal Gaussian shapes. These results were likewise established in References 13. and 22.

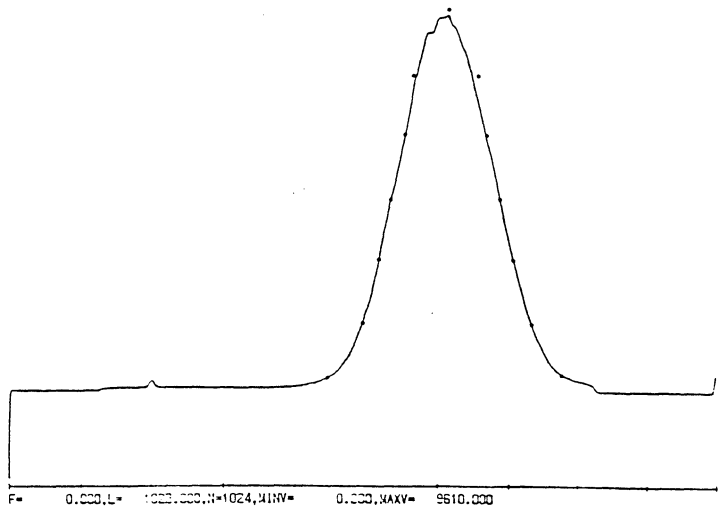

Fig. 4.15. Dye profile compared with a Gaussian shape (dots).

The shapes of the dye laser profile when inserting prisms in the cavity were calculated to be more Gaussian than Lorentzian but no perfect fittings were obtained.

4.5. SUMMARY

It has been shown that it is indeed possible to achieve spectral condensation by inserting prisms in the cavity of a dye laser. Studying Table 4. it seems as if employing two or three prisms would yield a dye laser bandwidth of 10-15 cm^{-1} useful in CARS experiments. The increase in spectral intensity, i.e. the decrease in energy divided with the decrease in FWHM when inserting prisms, reached its maximum when two prisms were employed.

Table 4. Summarizing the effects on a dye laser when inserting prisms.

NUMBER OF PRISMS	FWHM (cm^{-1})	ENERGY (mJ)	INCREASE IN SPECTRAL INTENSITY
0	86,9	5,5	—
1	24,6	3,8	2,4
2	12,5	2,7	3,4
3	9,3	1,5	2,6

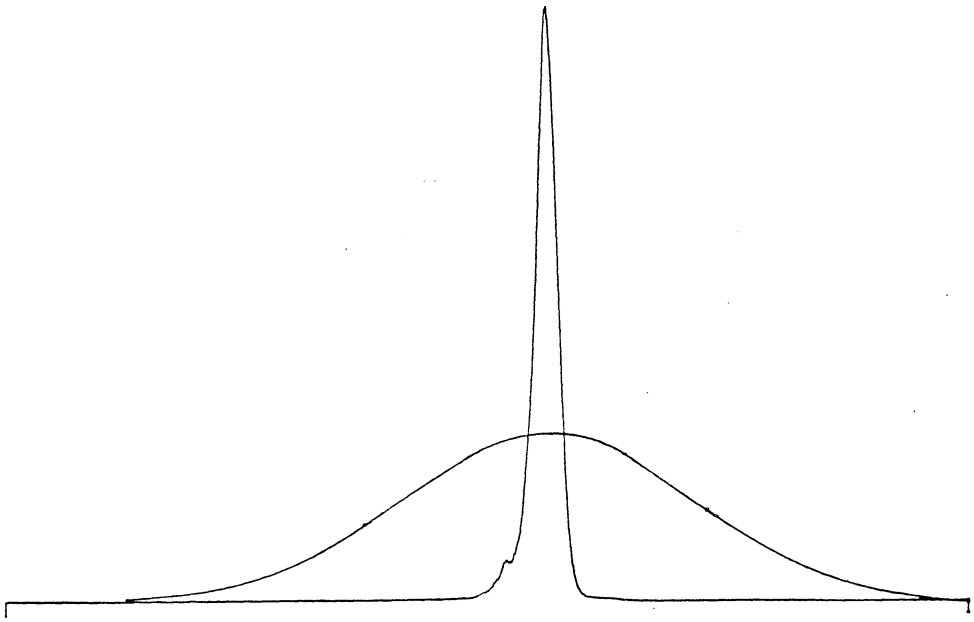

Fig. 4.16. Visualizing the effect on the dye laser output when inserting two F2-prisms in the cavity.

4.6 FUTURE PROJECTS

As for the future there are vast plans of installing prisms in a commercial dye laser and investigate the behavior of this laser. A special prism holder is about to be built for this purpose. It will also enable further experiments with the vertical arrangement of the prisms.

5. SHORT CAVITY

5.1. EXPERIMENTAL IDEA

In an optical resonator formed by two mirrors a infinitive set of eigenfrequencies (longitudinal modes) separated in frequency by an amount of c/2l occurs [18,25-30] where l is the optical length of the resonator and c is the speed of light. The number of frequencies which oscillates is limited by the bandwidth $\Delta\nu$ over which the laser gain exceeds the loss of the resonator. A typical laser output spectrum is illustrated in Fig. 5.1.

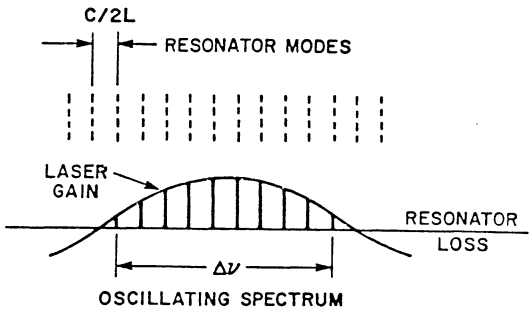

Fig. 5.1. The spectral contents of a laser operating on a single traverse mode and a number of different longitudinal modes.

Translated to wavelength the mode separation is:

$$\Delta\lambda = \frac{\lambda^2}{2\ l}$$

were λ is the lasing wavelength.
Using a short cavity, l < 25 mm, it is possible to resolve the longitudinal modes using a 5 m-spectrograph with a resolving power of 0.277 Å/mm. It is desirable to attain mode separations of 8 cm^{-1} for measurements and referencing in CARS [5], i.e. overlapping the rotational transitions, see Fig. 2.5., with the longitudinal modes, or with multiples of modes, of a dye laser. Referencing is used to compensate for the shot-to-shot variations in the dye laser spectral profile.

5.2. EXPERIMENTAL SET-UP

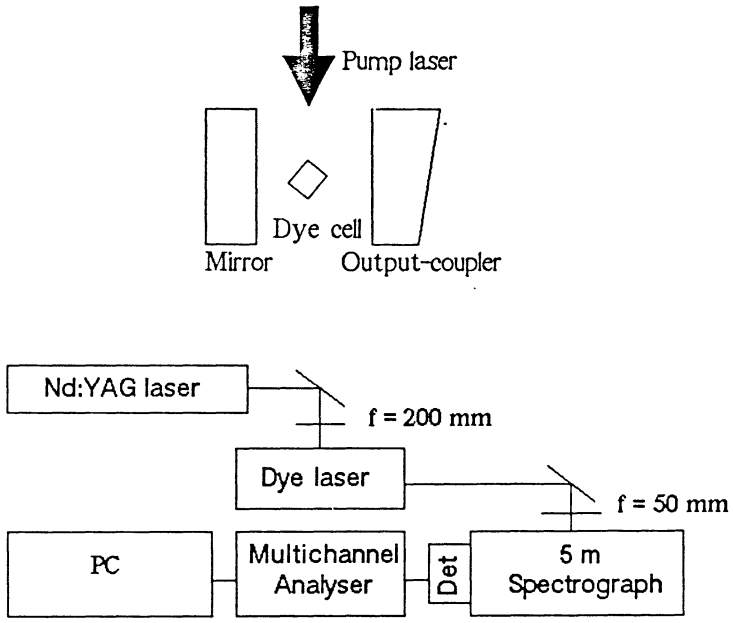

Fig. 5.2. The experimental set-up.

The experimental set-up is schematically shown in Fig. 5.2. The cavity consisted of a rear mirror, a dye cell and a wedged output-coupler. The rear mirror was a maxbrite mirror with a minimum reflective power of 99%. The quadratic (3mm) dye cell was made of quartz glass and tilted at Brewster's angle to attain vertically polarized laser light from the dye cell and to eliminate Fabry-Perot effects from the parallel walls of the cell. The dye flow was horizontal. KITON RED 620 dissolved in EtOH, yielding a concentration of 130 mg/l, was used as dye. The output-coupler was a wedged glass window. The dye cell was pumped from above by a Nd:YAG laser (532 nm), pulse energy : 12 mJ, focused with a cylindrical f=200 mm lens. Otherwise the pumping arrangements were much the same as described in the previous experiment. The laser output beam was directed by two mirrors and made divergent by a 50 mm lens focused on the slit of a 5 m-spectrograph with a dispersion of 0.277 Å/mm, working in the 9th order. For detection a Tracor-Northern diode-array detector TN-1710 was used. The signals were stored on a PC.

5.3. THE RESOLVING POWER OF THE DIODE ARRAY

To test the resolving power of the diode array, the following measurements were made [31]:

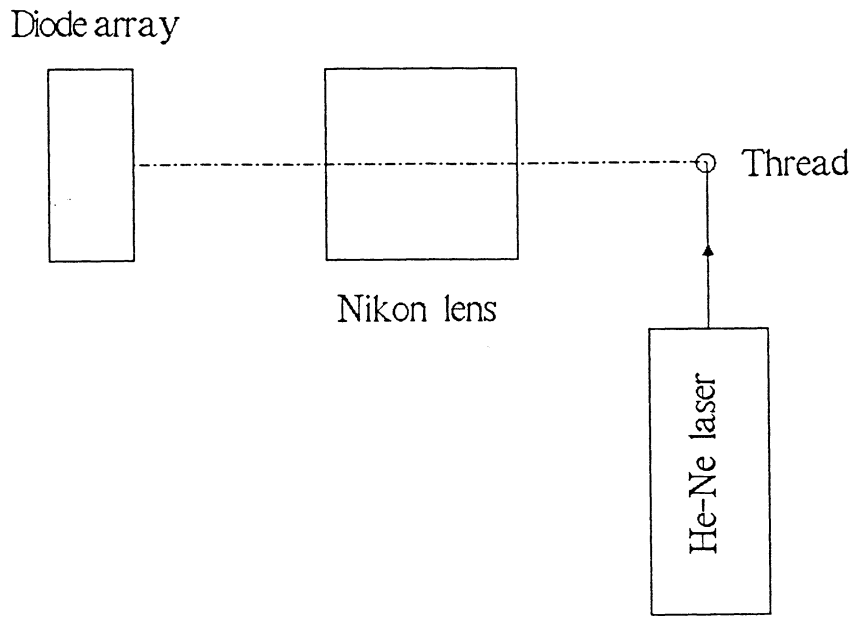

Fig. 5.3. The set-up for testing the resolving power.

The set-up is shown in Fig 5.3. A metallic thread, diameter 2.5 μm, was illuminated with a He-Ne laser. The illuminated area was then reproduced 1 to 1 by a Nikon f=50 mm lens on the diode array. The width of one pixel on the diode array was 25 μm i.e. much broader than the reproduced illuminated area. The FWHM was measured to be 4 channels on the multichannel analyser. To test the spectrograph the detector was mounted onto the spectrograph and a single-mode Nd:YAG laser beam was directed into the spectrograph. The FWHM was measured to be 4 channels. This showed that the diode array was the factor limiting the resolving power of the system, consisting of the spectrograph and the optical multichannel analyser.

5.4. CALIBRATION

In order to determine the dispersion of the system, the two sodium lines D_1 and D_2 were used. The light from a sodium lamp was focused on the slit of the spectrograph by a lens with a focal length of 40 mm. The highest visible order of the spectrograph was the 10th, but only one line was visible at a time on the OMA. Therefore the 9th order was chosen where both lines were visible and the resolving power was not reduced compared to the 10th order. The spacing between the two peaks were 0.5970 nm, corresponding to 551 channels, giving a dispersion of $1.08 \cdot 10^{-3}$ nm per channel. The FWHM of the sodium peaks were 6 channels, corresponding to 0.0065 nm.

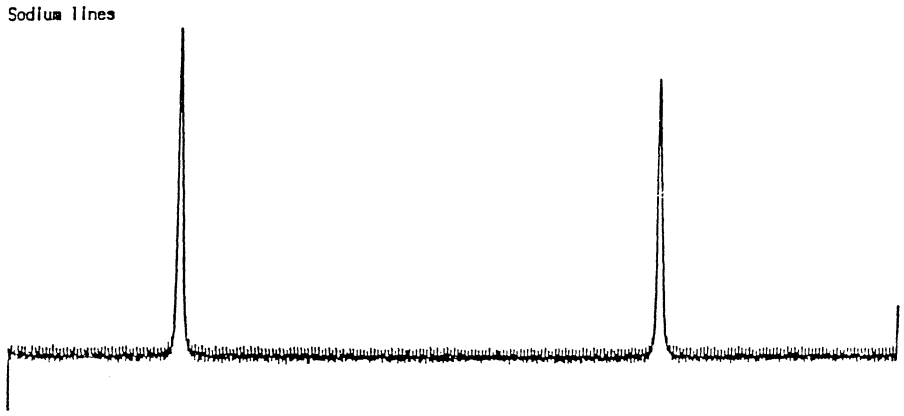

Fig. 5.4. The two sodium lines D_1 and D_2

5. MEASUREMENTS AND RESULTS

5.5.1. THE INFLUENCE OF CAVITY LENGTH ON MODE SEPARATION

The effect of the cavity length on the mode separation was measured. The distance between the mirrors were adjusted and measured. Then the cavity was lined up with a He-Ne laser. The output coupler and the rear mirror were adjusted to be parallel. The pump laser beam was then adjusted and focused on the dye cell by a cylindrical f=200 mm lens. To obtain lasing, the rear mirror was adjusted. The laser beam was then guided to the 5m-spectrograph by two mirrors. Fig. 5.5. shows a typical spectrum with the mode separation clearly visible.

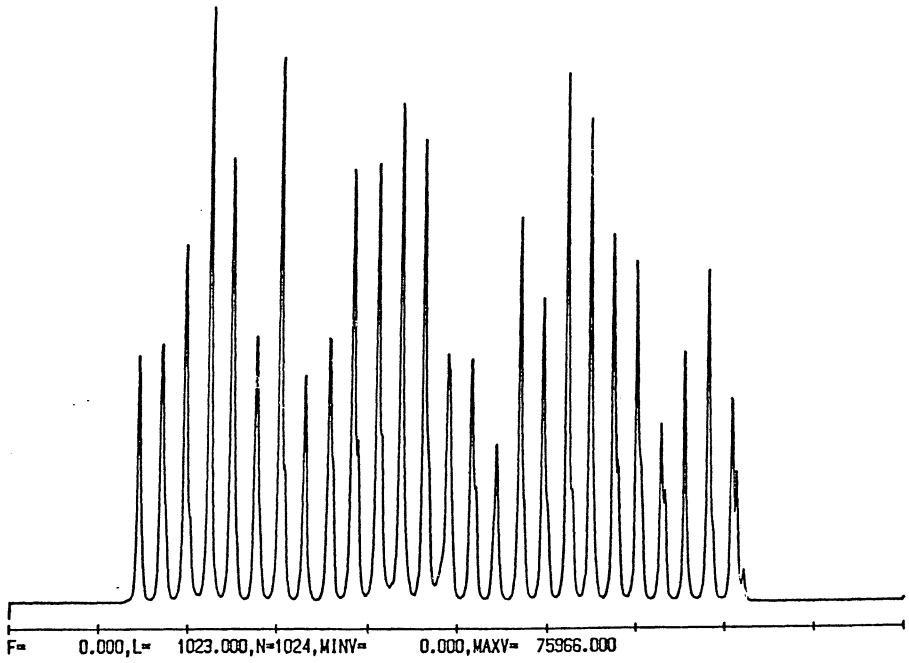

Fig. 5.5. The spectrum corresponding to a cavity length of 4.2 mm; 100 scans, exp.time: 100 ms.

As the cavity length varied from 4.2 mm to 25 mm the measured distance between the longitudinal modes in the lasing spectra were found to fit well with the free spectral length $\Delta\lambda$ of the cavity, this range being given by the well known expression

$$\Delta\lambda = \frac{\lambda^2}{2\,n\,l}$$

were λ is the radiant wavelength (5890 Å) and $n \cdot l$ is the optical path length.
Measurements were also performed with a cavity length up to 65 mm, but the resolving power of the OMA (4.33 mÅ) limited the measurements to a cavity length of 25 mm corresponding to a free spectral range of 5.40 mÅ.

Tab. 5. Experimental and theoretical values of the mode separation.

	Mode separation	
Cavity length	Experimental	Theoretical
4.2 mm	0.294 Å	0.320 Å
8.0 mm	0.187 Å	0.191 Å
9.0 mm	0.158 Å	0.172 Å

5.5.2. SINGLE-, MULTI-MODE PUMPING

The effect of single-mode and multi-mode pumping, respectively, were investigated. The FWHM of one of the longitudinal modes was measured to be 4 channels, corresponding to 4.33 mÅ, for single-mode pumping, and 6 channels, corresponding to 6.50 mÅ, for multi-mode pumping. The results for single-mode pumping is uncertain, due to the resolving power of the spectrograph. No difference in output power was measured.

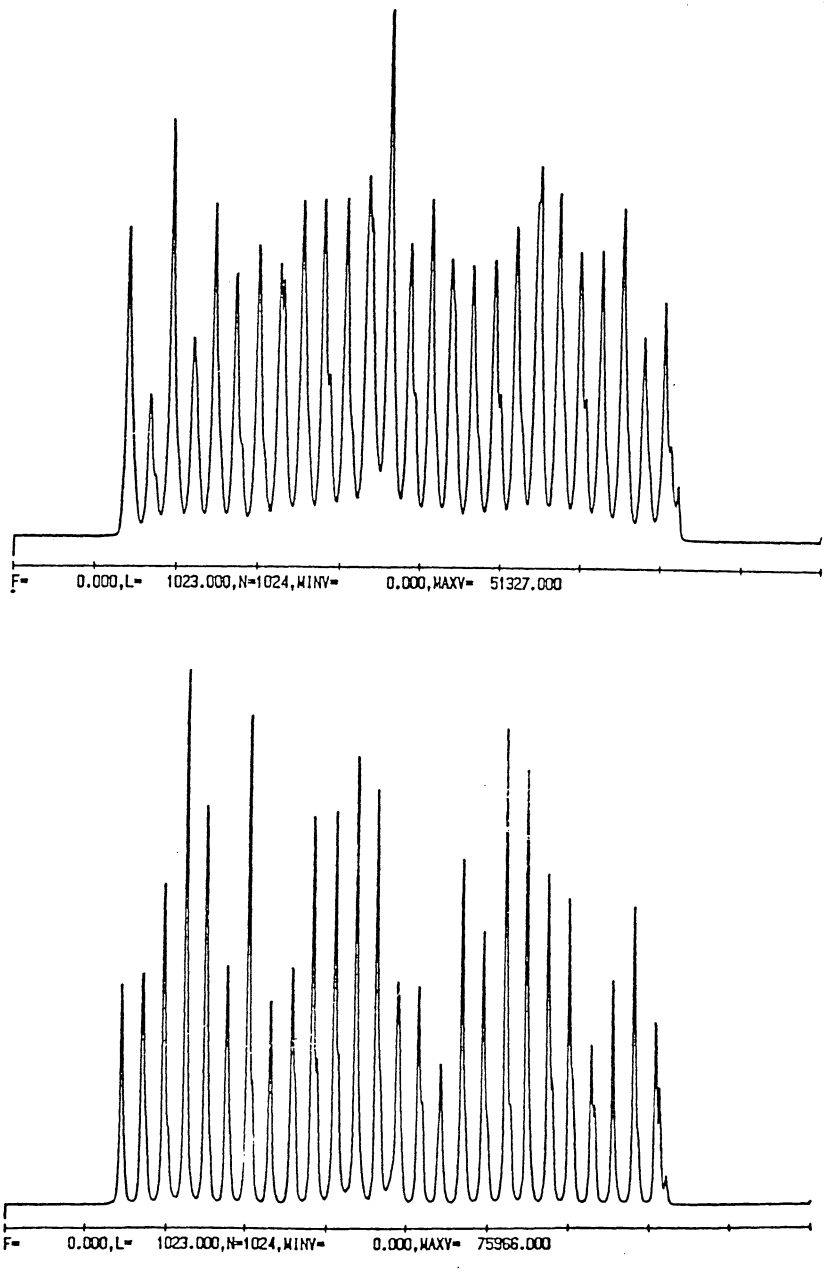

Fig. 5.6. a) Spectrum of multi-mode pumping and b) single-mode pumping. 100 scans, exposure time: 100 ms.

5.6. SUMMARY AND DISCUSSION

It is shown that the mode separation $\Delta\lambda$ fits well with the above mentioned well known expression

$$\Delta\lambda = \frac{\lambda^2}{2\ n\ l}$$

By adjusting the cavity length, l, the mode separation can be altered to the requested value. A practical problem occurs when trying to adjust the cavity length without changing the parallelism of the mirrors.

It is also shown that pumping the dye with a single-mode laser will decrease the FWHM of the longitudinal modes of the dye laser compared to multi-mode pumping. Exactly how much the declination is, is hard to tell due to the, in this case, poor resolving power of the MCA.

No differences concerning output power is measured for single- or multi-mode pumping.

6. ACKNOWLEDGEMENTS

We wish to thank Sara Agrup for not baking her now world-wide known banana cakes too often..., and David Nilsson the man who fled the country because Lund was too small for the three of us. Thank you Elna for not nagging about the most illicit use of your dear computer. Thanks Lenny S. for not wearing those corny shades, at least indoors; Anders Persson the lone ranger of the dark computer-jungle without whom we would not hawe tamed the mean machines; Christer Löfström, the best baby sitter of the entire institution, but also a hard working and famous scientist to be; Per-Erik Bengtsson, the coming golf star (handicap: 19). Thank you Ulf Westblom for sharing your treasure chamber with us and for your outstanding stamina; Marcus Aldén, our patient supervisor for flooding our poor minds with bundles of ideas and whims and helping us in every possible way. Thank you Sune S., the professor of professors, for your spiritual support.

7. REFERENCES

1. M. Aldén, "Applications of Laser Techniques for Combustion Studies", Lund Reports on Atomic Physics LRAP-22, 1983.

2. S. Svanberg, "Atom- och molekylspektroskopi", Lund, 1988.

3. S. Kröll, M. Aldén, T. Bergling and R.J. Hall, "Noise characteristics of single shot broadband Raman-resonant CARS with single- and multimode lasers", Appl. Opt. 26, 1068 (1987).

4. W.B. Roh, P.W. Schreiber and J.P.E. Taran, "Single-Pulse Coherent Anti-Stokes Raman Scattering", Appl. Phys. Lett. 29, 174 (1976).

5. H. Edner, "Application of laser spectroscopy to combustion and environmental probing", Lund Reports on Atomic Physics LRAP-77, 1987.

6. S. Kröll, M. Aldén, P.-E. Bengtsson and C. Löfström, "An Evaluation of Precision and Systematic Errors in Vibrational CARS Thermometry", 1983.

7. M. Aldén, K. Fredriksson and S. Wallin, "Application of a two color dye laser in CARS experiments for fast determination of temperatures", Appl. Opt. 23, 2053 (1984).

8. S. Kröll and D. Sandell, "Influence of laser-mode statistics on noise in nonlinear optical processes- application to single-shot broadband coherent anti-Stokes Raman scattering thermometry", Opt. Soc. Am. B5, 1910 (1988).

9. S. Kröll and D. Sandell, "A model for calculating the noise due to the stochastic nature of multimode laser radiation in nonlinear optical processes", (to appear in the proceeding from NLO'88).

10. D.A. Greenhalgh and S. T. Whittley, "Mode noise in broadband CARS spectroscopy", Appl. Opt. 24, 907 (1985).

11. M. Aldên, P.-E. Bengtsson and H. Edner, "Rotational CARS generation through multiple four-color interaction", Appl. Opt. 25, 4493 (1986).

12. M. Aldén, P.-E. Bengtsson, H. Edner, S. Kröll and D. Nilsson, "Rotational CARS: A Comparison of Different Techniques with Emphasis on Accuracy in Temperature Determination, 1988.

13. D. Nilsson, "Theoretical and Experimental Investigations of Rotational CARS as a Technique for Temperature Probing", Lund Reports on Atomic Physics LRAP-76, 1987.

14. F.P. Schäfer, Ed. "Dye lasers", F.P. Schäfer in Chapter 1, Springer-Verlag, 1973.

15. G.R. Fowles, "Introduction to Modern Optics", Chapter 9, Holt, Rinehart and Winston, 1975.

16. S. Borgström, "Laserfysik", Avd för Atomfysik, Lunds Tekniska Högskola, 1986.

17. B.A. Lengyel, "Lasers", Wiley-Interscience, 1971.

18. D.C. Hanna, Ed. "Principles of Lasers", O. Svelto, Plenum Press, 1982.

19. Spindler & Hoyer, "Dispersionsprismen", p. I1, 1987/88.

20. J.B. Breckinridge, "Optical Systems Engineering", California Institute of Technology, 1986.

21. E. Hecht and A. Zajac, "Optics", p. 43, 129-130, Addison-Wesley, 1974.

22. F.C. Strome, Jr. and J.P. Webb, "Flashtube-Pumped Dye Laser with Multiple-Prism Tuning", Appl. Opt. 10, 1348 (1971).

23. S. Murakawa, G. Yamaguchi and C. Yamanaka, "Wavelength Shift of Dye Solution Laser", Japan J. Appl. Phys. 7, 681 (1968).

24. F.J. Duarte, "Note on achromatic multiple-prism beam expanders", Opt. Comm. 53, 259 (1985).

25. B. Fan and T.K. Gustavsson, Appl. Phys. Lett. 28, 202 (1976).

26. F. Aussenegg and A. Leitner, Opt. Comm. 32, 121 (1980).

27. V.S. Smirnov, V.I. Studenov and V.A. Rozuvanova, Opt. Spectrosc. (USA) 56, 541 (1984).

28. H. Salzmann and H. Strohwald, Phys. Lett. A 57, 41 (1976).

29. J.A. Duncanson and W.S. Struve, J. Appl. Phys. 52, 3800 (1981).

30. A.J.Cox, Appl. Phys. Lett. 40, 664 (1982).

31. H.M. Hertz, M. Aldén and S. Svanberg, "Correction of Imaging Errors in Spatially Resolved Laser Scattering Experiments in Flames", Appl. Phys. B45, 33 (1988).

32. P. Ewart and D.R. Meacher, "A novel, widely tunable, single mode pulsed dye laser", Opt. Comm. 17, 197 (1989).

8. APPENDIX: HIGH TEMPERATURE AND PRESSURE CELL

INTRODUCTION

A cell is constructed by placing a small pipe oven in a pressure cell to fulfill the demands of CARS measurements at high pressures (15-20 bar) and high temperatures (1200 °C).

THE PRESSURE CELL

The pressure cell is constructed for very high pressures. The enclosed chamber has the shape of a cylinder with diameter 100 mm and the length of 100 mm. It consists of two gables screwed on to the main house, each gable has got a window of glass. On the house four windows are placed radially, see Fig. 1.

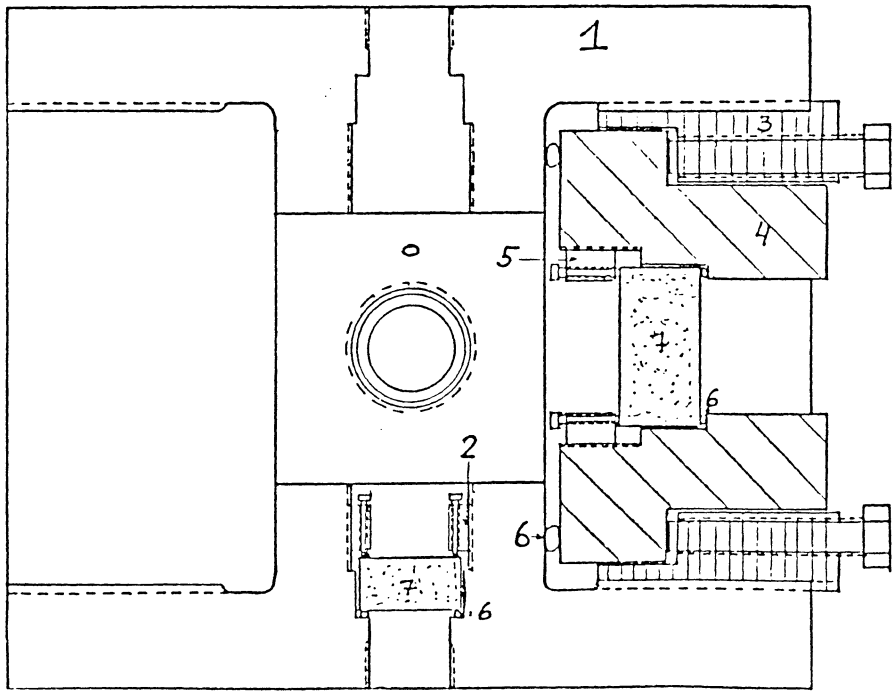

Fig. 1. The pressure cell. 1 bomb, 2 window holder , 3 gable holder, 4 gable with window, 5 window holder gable, 6 metallic o-ring, 7 quartz glass.

THE PIPE OVEN

The oven is placed inside the pressure cell. The oven is schematically shown in Fig. 2. A glow thread is winded around a ceramic pipe, diameter 15 mm, enclosed in insulation. To secure the electrical connections, another ceramic tube encloses the insulation package. The electrical connections consists of two metallic threads screwed in to the outer tube and taken out radially through the windows of the pressure cell. Thermal elements can be taken out radially through a window the same way. To prevent a too large temperature gradient two windows of safire glass are mounted on the ends of the inner pipe. The gas flow is led in to the oven cell and taken out the same way. The pipe oven is prospected and offerted by ENTECH.

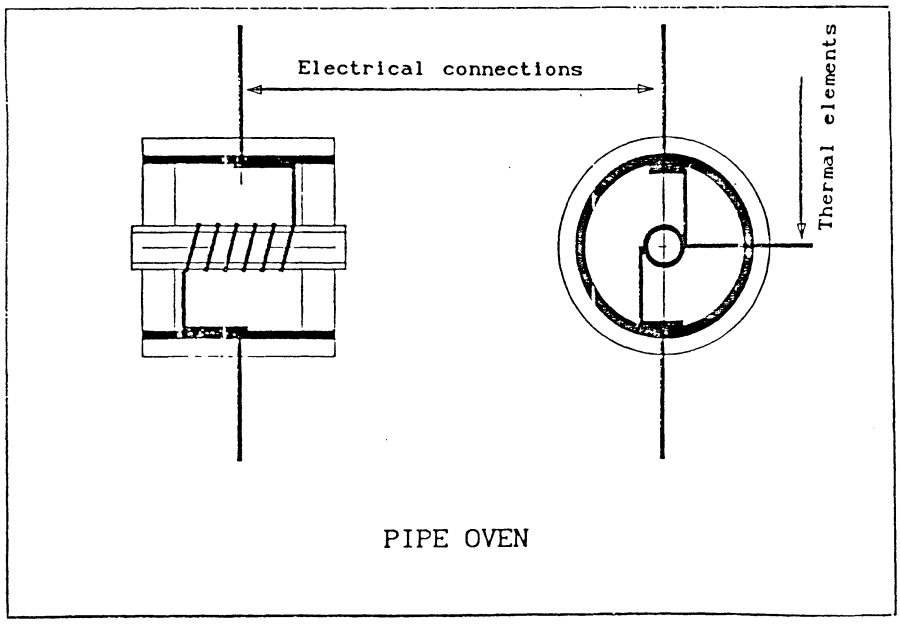

Fig.2. The pipe oven. Prospected by ENTECH.

ENTECH
ENERGITEKNIK AB

Ängelholm 1989-04-28

Er ref. Christer Löfström

Vår ref. S Alm

FÖRBRÄNNINGSTEKNISKT CENTRUM
Box 118
221 00 LUND

Offert rörugn för tryckkammare.

Med referens till Er förfrågan och diskussioner har vi härmed nöjet att erbjuda nedanstående ugn för temperatur upp till 1200 grad C.

1	st	Ugn med arbetsrör ca	15 mm innerdiameter
		Uppvärmd längd	50 mm
		Total längd	100 mm
		Effekt	ca 150 W
		Spänning	220 V en fas
		Max temperatur	1200 grad C

Ugnens utförande framgår av bifogade skiss. Elementanslutningar sker med skruvförbindning så att ugnskroppen kan föras in axiellt i tryckkammaren För styrning av ugnen lämnas två alternativ enligt nedan:

Tyristorstyrning på transformatorns primärsida. Regulator typ Eurotherm 815 S el motsvarande. Termolelement typ S

Pris 27.400:-

ON-OFF styrning på transformatorns primärsida. Regulator typ ERO FQV eller likn.

Pris 20.550:-

Leveranstid	ca 8 arbetsveckor från order
Leveransvillkor	Fritt Ängelholm.
Betalningsvillkor	30 dagar netto från leverans och faktura
Offert giltig	t o m 88-08-01

Vi hoppas att denna offert skall vara av intresse för Er och vi ber Er kontakta oss om något skulle vara oklart.

Med vänliga hälsningar
ENTECH AB

Staffan Alm

Adress Klippanvägen S-262 00 Ängelholm
Telex: 8335086 ENTECH Teletex: 2401=8335086=ENTECH Telefax: 0431-41032
Telefon 0431-152 95
Bankgiro Skandinaviska Enskilda Banken, Ängelholm 49 07 93-7 Postgiro 708-4965